HHS Public Access

Author manuscript

Ann Biomed Eng. Author manuscript; available in PMC 2020 April 01.

Published in final edited form as:

Ann Biomed Eng. 2019 April ; 47(4): 1012–1022. doi:10.1007/s10439-019-02209-0.

Efficacy of sonothrombolysis using microbubbles produced by a catheter-based microfluidic device in a rat model of ischemic stroke

Adam J Dixon[1], **Jun Li**[2], **John-Marschner Robert Rickel**[1], **Alexander L. Klibanov**[1,3], **Zhiyi Zuo**[2], and **John A. Hossack**[1]

[1]Department of Biomedical Engineering, University of Virginia, Charlottesville, VA

[2]Department of Anesthesiology, University of Virginia School of Medicine, Charlottesville, VA

[3]Cardiovascular Medicine, University of Virginia School of Medicine, Charlottesville, VA

Abstract

Limitations of existing thrombolytic therapies for acute ischemic stroke have motivated the development of catheter-based approaches that utilize no or low doses of thrombolytic drugs combined with a mechanical action to either dissolve or extract the thrombus. Sonothrombolysis accelerates thrombus dissolution via the application of ultrasound combined with microbubble contrast agents and low doses of thrombolytics to mechanically disrupt the fibrin mesh. In this work, we studied the efficacy of catheter-directed sonothrombolysis in a rat model of ischemic stroke. Microbubbles of 10 – 20 μm diameter with a nitrogen gas core and a non-crosslinked albumin shell were produced by a flow-focusing microfluidic device in real time. The microbubbles were dispensed from a catheter located in the internal carotid artery for direct delivery to the thrombus-occluded middle cerebral artery, while ultrasound was administered through the skull and recombinant tissue plasminogen activator (rtPA) was infused via a tail vein catheter. The results of this study demonstrate that flow focusing microfluidic devices can be miniaturized to dimensions compatible with human catheterization and that large-diameter microbubbles comprised of high solubility gases can be safely administered intraarterially to deliver a sonothrombolytic therapy. Further, sonothrombolysis using intraarterial delivery of large microbubbles reduced cerebral infarct volumes by approximately 50% versus no therapy, significantly improved functional neurological outcomes at 24 hrs, and permitted rtPA dose reduction of 3.3 (95% C.I. 1.8 – 3.8) fold when compared to therapy with intravenous rtPA alone.

Author Contributions Statement

AJD, JAH, ZZ conceived of study. AJD wrote main manuscript text. AJD, JMRR, JL conducted experiments and analyzed data. JAH, ALK, and ZZ supervised the study and all authors reviewed the manuscript.

Competing Interest

Authors AJD and JAH are inventors listed on an issued patent (US Patent No. 9,895,158) that relates to some aspects of the content of this study.[56]

Introduction

Early recanalization of the large occluded arteries in the brain is an essential component of treatment after the onset of acute ischemic stroke. Intravenous administration of recombinant tissue plasminogen activator (rtPA) only achieves complete recanalization in approximately 30% of patients, a limitation that has motivated the development of alternative recanalization techniques.[1,2] Current generation of thrombectomy catheters, known as “stentrievers”, has recently achieved primary vessel recanalization rates approaching 90% and complete restoration of perfusion in distal capillary beds in close to 60% of cases.[3,4] These results, reported by multiple independent trials (MR CLEAN[5], SWIFT PRIME[3], ESCAPE[6], REVASCAT[7], EXTEND-IA[8]), represent a significant improvement over intravenous rtPA therapy and strongly support the use of interventional endovascular approaches for treating acute ischemic stroke patients.[9]

However, despite successful recanalization of the primary vessel, a subset of patients still fails to achieve clinical improvement. One possible explanation for this may be microcirculation no-reflow, a situation in which major vessel recanalization does not result in microvascular reperfusion.[10,11] Indeed, while improved outcomes of recent trials were strongly linked to improved recanalization rates, the 90-day outcomes of patients whose distal perfusion was not restored (i.e. thrombolysis in cerebral infarction (TICI) scores of 0/1/2a scores) were significantly worse than the outcomes of patients whose distal perfusion was completely restored (34% vs 48% with a functional 90-day modified Rankin Score, respectively, $p < 0.001$).[12,13] Therefore, given the recent success of stent retrievers for treating the primary occlusion, the focus must now turn to extending the “reach” of these catheters to address distal occlusions beyond the M2 segment of the middle cerebral artery (MCA) that contribute to poor revascularization in the remaining ~30% of ischemic stroke patients.

Multiple reports have suggested that the use of adjuvant ultrasound (with or without microbubbles) improves rtPA efficacy and distal reperfusion.[14–17] In a clinical trial, ischemic stroke patients treated with a combination of rtPA, transcranial ultrasound, and microbubbles had significantly higher rates of complete recanalization (55% vs 24%) and greater clinical improvement (54.9% vs 31.1%) compared with patients who received rtPA alone.[17] Notably, the observed rate of complete recanalization was similar to that achieved by the recent stentriever trials discussed above. However, a limitation of these sonothrombolysis-based approaches was an increased risk of off-target intracerebral hemorrhage, which led at least one clinical study to early termination.[18] Thus, methods must be developed to confine the effects of sonothrombolysis to the primary occluded vessel and its downstream capillary bed to limit these off-target deleterious effects in otherwise unaffected regions of the brain.

In this work, we evaluated a catheter-based sonothrombolysis treatment method that used large-diameter microbubbles for accelerating primary vessel recanalization in a rat model of ischemic stroke. The development of this method was informed by the clinical findings in support of endovascular interventions for acute ischemic stroke and the growing body of evidence indicating that larger microbubbles produce enhanced bioeffects due to increased

microstreaming,[19–22] increased momentum transfer via acoustic radiation force, [23–25] and higher-energy cavitation events.[26,27] Thus, we hypothesized that off-target hemorrhage could be mitigated by directing the delivery of microbubbles to the occluded blood vessel while enhancing the thrombolytic effect of sonothrombolysis by using larger microbubbles with enhanced bioeffects.

Methods

Animal protocols were approved by the University of Virginia ACUC (Animal Care and Use Committee). All experiments and methods were performed in accordance with the relevant guidelines and regulations.

Microfluidic device fabrication and microbubble production

Two flow-focusing microfluidic device (FFMD) designs were used in this study – a catheter-based FFMD sized to human-compatible dimensions that was used to establish feasibility of a translational, catheter-based therapeutic approach and a larger FFMD that was used to achieve high microbubble production rates for the *in vivo* studies. The larger FFMD was also equipped with an outlet port that could accept a PE-10 tube that was used to directly convey microbubbles from the FFMD to the rat's carotid artery in the *in vivo* experiments. The catheter-sized FFMD was too small to allow for this interconnect, but was too large to be operated directly within the rat's carotid artery.

Both FFMDs were fabricated from custom SU-8 molds and manufactured by photolithography, as previously described.[28,29] Devices were fabricated in polydimethylsiloxane (PDMS, Sylgard 184, Dow Corning) and were bound via oxygen plasma to a clean PDMS substrate. The microfluidic devices had channel heights between 20 and 22 micrometers and nozzle widths of approximately 8 micrometers. The gas and liquid channels were approximately 30 and 50 micrometers wide, respectively. All stated dimensions are accurate to ± 1 micrometer. A schematic of the catheter-based FFMD is shown in Figure 1, while a schematic of the larger FFMD and characterization of its operating conditions are provided in Figure 1 of Dixon *et al*[30]. The production rate and diameter measurements were acquired from a single FFMD operated on three separate days to gauge reproducibility.

Microbubbles were produced using 99.998% N_2 (GTS Welco, Richmond, VA) and a liquid phase of bovine serum albumin (4% w/v BSA) and dextrose (10% w/v) in 0.9% saline. The liquid phase was prepared by mixing its components overnight at 4 °C. The liquid phase was pressurized using a syringe pump and was filtered by 0.2 μm nylon filters prior to use (PhD 2000, Harvard Apparatus, Holliston, MA). A digital multimeter was used to regulate gas pressure (06-664-22, Fisher Scientific, Waltham, MA). In the larger FFMD, microbore PTFE tubing of 762 μm outer diameter was used to convey the gas and liquid phases into the device, while the catheter-based FFMD used fused silica capillary tubes (O.D. = 110 μm, Polymicro, Molex Inc). Liquid flow rates varied between 30 – 90 μL/min and gas pressures varied between 43.8 and 89.6 kPa. The microbubbles used in the sonothrombolysis studies had a nominal diameter of 15 μm. This size is in the middle of the microbubble diameter range that this FFMD design can produce (approximately 8 – 25 μm), and was empirically

determined to be the most efficacious in prior *in vitro* sonothrombolysis experiments.[30] Microfluidic microbubble production was monitored by a high-speed camera (SIMD24, Specialised Imaging, Tring, UK) mounted to an inverted microscope (Olympus IX53), and production rate and diameter were measured in ImageJ 1.7.0 (National Institutes of Health [NIH]).

Dose tolerance study of intraarterially administered microbubbles

Prior to conducting the ischemic stroke studies described below, a study was performed to determine the intraarterial microbubble dose below which no gas embolism or cerebral infarction was observed. On the day of surgery, male Sprague-Dawley rats were anesthetized with 5 vol% isoflurane in medical air, intubated, and ventilated artificially throughout the experiment using an anesthesia ventilator. Isoflurane was reduced to 2 vol% in medical air after intubation for the remainder of the experiment. The right external carotid artery (ECA) was catheterized and a PE-10 tube was inserted to the junction of the ECA and the right internal carotid artery (ICA). Microbubbles of approximately 15 μm diameter produced at three different production rates were administered continuously to the rat ECA through the PE-10 tube for 15 minutes. The production rates studied were: 150×10^3, 500×10^3, and 1.2×10^6 MB/s (corresponding to injected gas volumes of approximately 240, 800, and 1900 μL). A control group that underwent the catheterization procedure with a 2 mL saline injection (sham) was also performed (N = 3 rats in all groups, rat weight between 425 – 500 g).

Rats were monitored for changes in respiration or heart rate during microbubble administration. After 15 minutes of microbubble administration, rats were removed from anesthesia and a neurological deficit score (NDS) was evaluated immediately after recovering from anesthesia and 24 hours later.[31] After 24 hours, rats were sacrificed and their brains were fixed in paraformaldehyde for 12 hours. The brains were sliced into 2 mm thick sections and were stained with triphenyltetrazolium chloride (TTC). Brain infarct volume in TTC-stained slices and NDS scores were evaluated by an anesthesiologist who was blinded to the study groups.

Neurological deficit scoring system

The neurological deficit scoring (NDS) system is as follows: 7, dead; 6, unresponsiveness to stimulation and with depressed level of consciousness; 5, walking only if stimulated; 4, circling or walking to the left; 3, spontaneous movement in all directions, contralateral circling only if pulled by the tail; 2, decreased grip of the left forelimb; 1, failure to extend left forepaw fully; 0, no apparent deficits.[31]

Rat model of ischemic stroke

On the day of surgery, rats were anesthetized with 5 vol% isoflurane in medical air, intubated, and ventilated artificially throughout the experiment using an anesthesia ventilator. Isoflurane was reduced to 2 vol% in medical air after intubation for the remainder of the experiment. Venous blood from a donor rat was clotted in a PE-50 tube and maintained at 4°C for up to 48 hr prior to experimentation. Ischemic stroke was simulated by injecting the clot into the right middle cerebral artery (MCA) via ECA catheterization, as

described above. The clot was administered via a PE-10 tube and was left undisturbed for 15 minutes prior to the application of a therapeutic intervention. The total volume of clot administered to each rat was the same and was measured to be approximately 16 μl. A schematic of the catheterization and location of clot placement is depicted in Figure 2A, ultrasound Doppler images (acquired with 15L8 probe on Acuson Sequoia) demonstrating reduced blood flow following clot placement are shown in Figures 2B, 2C, and excised brains showing the location of the clot and the occluded MCA are presented in Figures 2F and 2G.

As described in Table 1, animals were randomized to four different therapeutic interventions. Animals in all groups underwent ECA catheterization and received a tail-vein catheter. Animals in Groups A, B, and C did not undergo sonothrombolysis treatment and instead received a 500 μl sham injection of saline into the ECA. All rtPA was administered over the course of 30 mins, with a 10% initial bolus, via the tail vein catheter at doses listed in Table 1. This rtPA administration technique mimics clinical protocols and is intended to maintain rtPA concentration in the approximately linear range of is dose-response curve.[32] Note that 0.9 mg/kg rtPA was considered to be comparable to a human clinical dose.[33]

Group D animals received microbubbles produced by the benchtop-FFMD through the ECA catheter. The microbubble outlet channel of the FFMD was connected directly to the ECA catheter to convey microbubbles into the ECA catheter. Following injection of the clot, the hair on the rat's head was removed to expose the bare skin to facilitate acoustic coupling. The brain was imaged using color Doppler (Fig 2B–E) to confirm that the clot was lodged upstream of the MCA, and a single-element therapeutic ultrasound transducer was placed on the skull so that its unfocused beam would broadly insonate the area of the MCA that contained the clot. Therapeutic ultrasound was administered by a 1 MHz center frequency, unfocused, single element ultrasound transducer that was coupled to the skull by ultrasound gel (V302-SU, Olympus Panametrics, Waltham, MA). Ultrasound energy was applied at a 10% duty factor in bursts of 100 cycles with a peak negative pressure of 500 kPa (as measured in a water tank). Ultrasound was applied continuously, while microbubbles (15 μm diameter, production rate of 250×10^3 MB/s) were injected for 30 s every 4.5 minutes. The intermittent dosing approach resulted in a maximum injected gas volume of approximately 80 μL. This combined therapy was administered for a total of 30 min. Microbubble injection was not continuous because the catheter blocked blood flow to the brain, and blood flow could not be blocked for the entire 30-minute intervention. All microbubble production rates quoted in the rat studies were accurate to approximately ± 20 %, while all microbubble diameters stated for the rat studies were accurate to approximately ± 1 μm.

Following the application of sonothrombolytic therapy, catheters were removed and the rats recovered from anesthesia. NDS was measured immediately after waking from anesthesia and 24 hours after the therapeutic intervention.[31] The neurological deficit was also evaluated 24 hr after the intervention. After 24 hours, rats were sacrificed and their brains were fixed in paraformaldehyde for 12 hours. The brains were sliced into 2 mm thick sections and were stained with triphenyltetrazolium chloride (TTC). Brain infarct volume in TTC-stained slices and NDS scores were evaluated by an anesthesiologist who was blinded to the study groups.

Statistical Analysis

For continuous, normally distributed data, statistical significance among experimental groups was determined using a 1-way ANOVA and Tukey-Kramer multiple comparisons test with $\alpha = 0.05$. Statistical significance of non-normally distributed data and categorical data were evaluated using Wilcoxon-Mann-Whitney tests with $\alpha = 0.05$. Data and additional details related to statistical analyses are available upon request.

Results

Microbubble production by catheter-based FFMD

A schematic of the catheter-based FFMD channel geometry is illustrated in Figure 1A,B. The footprint of the microfluidic channels were 540 μm wide and 3020 μm long, while the narrowest channels were 25 μm wide. The overall dimensions of the FFMD on the distal end of the catheter were approximately 1.0 mm wide, 0.6 mm tall, and 5.5 mm long. MBs of diameters between 8.5 and 28.0 μm were produced at rates between 5.6×10^3 and 118×10^3 MB/s. Gas pressures ranged from approximately 40 to 90 kPa and liquid flow rates were varied between 20 and 60 μl/min (Fig 1 E,F). For reference, the larger FFMD used in the rat studies was previously characterized and produced MBs of diameters between approximately 8.5 and 31 μm at rates between approximately 90×10^3 and 1.2×10^5 MB/s.[30] The production rate of the catheter-dimensioned FFMD was limited by the strength of the PDMS-PDMS bonds, which typically failed when the liquid flow rate exceeded 60 μl/min.

Dose tolerance assessment of intraarterially administered microbubbles

Infarct volumes caused by gas embolization of the cerebral vasculature were evaluated to assess damage caused directly by microbubble administration. TTC-staining results for a single rat brain in each of the three dosing groups are shown in Figure 3. Rats that received the highest MB doses exhibited minor areas of localized infarct on the side of the brain that was catheterized. Rats that received the lowest MB dose and no MBs showed no signs of gross infarct. Rats that received a medium dose of microbubbles exhibited an average of 6.6 ± 2.7 % infarct volume. One rat that received a high dose of microbubbles exhibited 13.7 % infarct volume, while a second rat that received the same dose exhibited respiratory distress and died approximately 4 hours after microbubble administration. All rats that were alive at 24 hours had a NDS of 0, except one rat that received the highest dose of microbubbles, which had a NDS of 2.

Rat ischemic stroke model

No rats were observed to exhibit cardiac or respiratory distress due to administration of ultrasound or microbubbles. No rats exhibited intracranial bleeding or other signs of gross hemorrhage as would be observed in the histology prior to TTC staining.[34] Our analysis did not screen for microhemorrhage, which could have resulted from the aggressive sonothrombolysis treatment.

Infarct volumes were evaluated for rats in each experimental group. Representative TTC staining results are presented in Figure 4 and quantitative infarct volumes and NDS scores are depicted as box plots in Figure 5. Infarct volumes for each experimental group were

(mean ± std. dev.): control − 60.6 ± 19.7 %, low dose rtPA (0.09 mg/kg) – 63.6 ± 22.0%, high dose rtPA (0.9 mg/kg) – 23.3 ± 15.9%, and sonothrombolysis plus low dose rtPA (0.09 mg/kg) – 32.3 ± 20.1 %.

The infarct volume results for the control and low-dose rtPA groups were not significantly different ($p = 0.392$). The infarct volumes for the high dose rtPA group was significantly different from the control ($p = 0.0121$) and low-dose rtPA groups ($p = 0.006$), but not the sonothrombolysis group ($p = 0.805$). The infarct volumes for the sonothrombolysis group was significantly different only from the low-dose rtPA group ($p = 0.048$), but not from the control group ($p = 0.089$) or high-dose rtPA group ($p = 0.805$).

The average NDS measured at 24 hr post-intervention for Groups A, B, C, and D were also evaluated for statistical significance. The NDS results for the control and low-dose rtPA groups were not significantly different ($p = 0.341$). The NDS for the high dose rtPA group was significantly different from the control group ($p = 0.001$), but not the low-dose rtPA ($p = 0.073$) or the sonothrombolysis group ($p = 0.899$). The NDS for the sonothrombolysis group was significantly different from both the control ($p = 0.001$) and low-dose rtPA groups ($p = 0.047$), but not from the high-dose rtPA group ($p = 0.805$).

The experiment was designed to permit the calculation of a rtPA dose response, using the low-dose rtPA and high-dose rtPA groups to establish the effect-size of increasing rtPA dose. The measured infarct volume was assumed to scale linearly with increasing rtPA dose, such that the infarct volume decreased from 63.6 ± 22.0% at 0.09 mg/kg to 23.3 ± 15.9% at 0.9 mg/kg, corresponding to a reduction of 4.9 ± 0.9 % per each additional 0.1 mg/kg injected dose. The sonothrombolysis group exhibited an infarct volume of 32.3 ± 20.1 %, representing a decrease of 31.3 ± 29.8% relative to the low dose rtPA group. Based on the assumed linear relationship between rtPA dose and fibrinolysis rate,[32] the introduction of sonothrombolysis was equivalent to the effect of an additional rtPA dose of 0.63 ± 0.18 mg/kg. This equates to a potential rtPA dose reduction of 3.3 – fold (95% C.I.: 1.8 – 4.8) required to reach the performance of 0.9 mg/kg rtPA. Put another way, sonothrombolysis plus approximately 0.27 ± 0.18 mg/kg rtPA would be expected to match the performance of 0.9 mg/kg rtPA in this experimental model.

Discussion

The primary aim of this study was to evaluate the *in vivo* dose tolerance and efficacy of large-diameter microbubbles produced by a FFMD for sonothrombolysis applications. Microbubbles of similar composition and origin have previously been evaluated for sonoporation-mediated *in vitro* drug delivery[28,29], *in vivo* contrast enhancement in a murine model,[35] and *in vitro* sonothrombolysis of human blood clots.[30] In prior sonoporation studies, microfluidically-produced microbubbles with N_2 gas cores, weak-stabilizing shells, and diameters greater than 10 μm were observed to induce sonoporation-mediated drug delivery at peak negative pressures that were significantly lower than pressures that are widely reported to induce sonoporation with smaller, lipid shelled microbubbles of 1 – 4 μm diameter.[29,36–38] These observations were corroborated by other findings that suggested larger microbubbles elicited stronger bioeffects than smaller microbubbles in the context of

multiple therapeutic applications, including sonoporation,[36] blood brain barrier disruption,[39] and sonothrombolysis studies.[30,40] Notably, these other studies compared microbubbles of 1 – 2 μm diameter to microbubbles of 2 – 4 μm diameter but did not evaluate larger microbubbles, presumably due to embolic risk associated with large diameter, long-circulating microbubbles. Despite this limitation, however, significantly greater bioeffects were observed when using larger size microbubble populations.

The motivation to evaluate even larger microbubbles for therapeutic applications stems from the observations stated above and the understanding that larger microbubbles produce enhanced bioeffects due to increased microstreaming,[19–22] increased momentum transfer via acoustic radiation force,[23–25] and higher-energy cavitation events.[26,27] Sonothrombolysis is a natural application for enhanced therapeutic efficacy derived from large diameter microbubbles because thrombolytic therapy must be administered quickly and, if possible, with as little thrombolytic agent as is necessary to reduce the risk of severe off-target bleeding. Until now, the primary limitation for the use of large microbubbles for therapeutic applications has been the risk of gas embolism associated with microbubbles of diameters larger than the smallest lung capillaries. The innovation in this work is the catheter-based administration of microbubbles with short circulation half-lives derived from their composition of high solubility gases and a weak surfactant shell. In a previous study, these microbubbles were observed to exhibit average circulation half-lives of approximately 21 s when administered intravenously in a murine model, with almost all microbubbles observed to be cleared by the lungs with no respiratory or cardiac distress.[35]

Miniaturization of FFMDs to human-compatible dimensions

Most FFMDs used for microbubble production are relatively large (> 1 cm^2 footprint) and are designed to operate on the benchtop, with the intent of producing microbubbles for storage and later use.[41,42] Benchtop-scale FFMDs are capable of producing microbubbles in excess of 1×10^6 per second with diameters as small as 1.5 μm.[30,43] However, there is no feasible means of administering large-diameter microbubbles that rapidly dissolve aside from a catheter-based implementation. Thus, it was important to evaluate the feasibility of miniaturizing the FFMD to human-compatible dimensions. The catheter-based design is also intended for integration onto a catheter that emits therapeutic levels of ultrasound energy via either a forward-looking[44] or radially-emitting ultrasound transducer[45] and contains on-chip sensors for real-time monitoring and control of microbubble production rate and diameter.[46] The present study focused on ischemic stroke, but a multi-function sonothrombolysis catheter could find application in stroke, deep vein thrombosis, myocardial infarction, and other thrombosis-related conditions including those pertaining to the microvasculature.[47–51] Overall, the peak production rate of approximately 100×10^3 MB/s achieved by the PDMS catheter-based FFMD is probably sufficient for future translation, with the possibility of increased production rates achievable by using a more robust design.

Dose tolerance of intraarterial microbubble administration

The dose tolerance of intraarterial administration of large diameter, microfluidically produced microbubbles was evaluated to determine a suitable dosing range in the rat model. Microbubbles were administered continuously for 15 min, with total injected N_2 gas

volumes of approximately 240 μl, 800 μl, or 1910 μl. Small, localized infarct zones were observed to result from gas emboli in rats receiving 800 and 1910 μl N_2 doses, while no gross infarct or neurological deficit was observed at the lowest dose. These results are broadly in line with those of Helps *et al*, who observed that rapid injection of 400 μl air into the rabbit cerebral vasculature resulted in disrupted cerebral blood flow for approximately 180 min, but caused no lasting neurological effect.[52] Their dose corresponded to roughly 180 μl/kg, which is less than the lowest dose studied in this rat model – 600 μl/kg. Although, the discrepancies between injection duration (immediate versus 15 min) and animal models (rabbit versus rat) make direct comparisons difficult, there is precedent for intraarterial injection of gas volumes on this order of magnitude.

In the stroke model, microbubbles were administered directly to the occluded blood vessel via a catheter placed at the junction of the ICA/ECA. It was our intent to simulate the targeted clinical condition in which a catheter would be placed directly in the occluded vessel of a stroke patient. A limitation of using the rat model was that microbubbles could not be administered continuously, as the catheter occluded blood flow towards the brain and prevented microbubbles from reaching the clot while the catheter was in place. Accordingly, large doses of microbubbles were administered for 30 s every 4.5 min over the course of the 30 min procedure. The selection of this dosing pattern was based on the time required for the ICA to completely clear of microbubbles, which indicated that the microbubbles had either dissolved or migrated towards the clot and out of view of the surgical microscope. In total, approximately 80 μl of gas was administered in the stroke animals, which was less than the lowest dose evaluated in the dose tolerance study.

A potentially confounding factor when evaluating the safety of these microbubbles is the interaction between the microbubbles and the ultrasound excitation required for sonothrombolysis therapy. In response to therapeutic ultrasound, secondary radiation-forces can promote coalescence of aggregated microbubbles into larger microbubbles,[53] which may reduce the safety profile of microbubble-mediated therapies. More investigation is required to evaluate the impact of these effects in the context of ischemic stroke therapies, but ultrasound-induced formation of very large diameter microbubbles may be a limitation of microbubble formulations that exhibit low-stability and rapid gas exchange

Sonothrombolysis and rtPA dose reduction

The infarct volume and neurological deficit results of the stroke study indicated that the sonothrombolysis treatment with 0.09 mg/kg rtPA (approximately $1/10^{th}$ clinical dose) was more effective than 0.09 mg/kg rtPA but was not as effective as 0.9 mg/kg rtPA. This was the expected result of this study's design and permitted the calculation of the effective rtPA dose-reduction enabled by the sonothrombolysis treatment method. As stated in the results, sonothrombolysis using the large diameter, transiently stable microbubbles permitted a dose reduction of approximately 0.63 ± 0.18 mg/kg, corresponding to a 3.3-fold (95% C.I.: 1.8 – 4.8) dose reduction. This quantitative analysis relies on the assumption that the rtPA dose response is approximately linear in the 0.09 to 0.9 mg/kg range used in this study. rtPA doses in this range correspond to average blood concentrations of between approximately 2 – 20 μM, which are in the linear range of the empirically determined relationship between

rtPA concentration and fibrinolysis rates.[32] This degree of rtPA dose reduction is noteworthy because many stroke patients are contraindicated for rtPA due to bleeding risks and are therefore left with limited treatment options (fewer than 5% of ischemic stroke patients receive rtPA).[54] Therefore, it is the goal of many interventions to either eliminate or greatly reduce the required rtPA dose.

Analysis of brain cross-sections before and after TTC staining indicated that no major hemorrhagic events occurred in any of the rats. Although the rat model used in this study did not permit the detection of microhemorrhages, the lack of observable macroscopic hemorrhage provides preliminary support for the hypothesis that this particular sonothrombolysis regimen may be administered without significantly increasing the risk of gross hemorrhagic transformation. Further, the addition of sonothrombolysis to the low-dose rtPA treatment resulted in significant recanalization of not only the primary vessel, but also the distal vasculature, as can be seen from the TTC staining results. Localized regions of the most distal vasculature were still occluded, perhaps from either clot fragments or gas emboli, and resulted in permanent tissue loss, but at a much lower incidence when sonothrombolysis was applied. Taken together, the lack of gross hemorrhage and significantly improved perfusion of the distal capillary bed are promising early results of this potential therapy.

Acknowledgements

Partial support for this research is provided by the National Institutes of Health under NIH grants S10 RR025594 and R01 HL141752 to JAH and by a NSF GRFP fellowship to AJD. The content is solely the responsibility of the authors and does not necessarily represent the official views of the NIH or NSF.

References

1. Tissue plasminogen activator for acute ischemic stroke. The National Institute of Neurological Disorders and Stroke rt-PA Stroke Study Group. N. Engl. J. Med 333, 1581–1587, (1995). [PubMed: 7477192]
2. Bhatia R et al. Low rates of acute recanalization with intravenous recombinant tissue plasminogen activator in ischemic stroke: real-world experience and a call for action. Stroke 41, 2254–2258, (2010). [PubMed: 20829513]
3. Saver JL et al. Stent-Retriever Thrombectomy after Intravenous t-PA vs. t-PA Alone in Stroke. New England Journal of Medicine 372, 2285–2295, (2015). [PubMed: 25882376]
4. Tomsick T TIMI, TIBI, TICI: I Came, I Saw, I Got Confused. AJNR Am J Neuroradiol 28, 382–384, (2007). [PubMed: 17297017]
5. Berkhemer OA et al. A Randomized Trial of Intraarterial Treatment for Acute Ischemic Stroke. New England Journal of Medicine 372, 11–20, (2015). [PubMed: 25517348]
6. Goyal M et al. Randomized Assessment of Rapid Endovascular Treatment of Ischemic Stroke. New England Journal of Medicine Epub, (2015).
7. Jovin TG et al. Thrombectomy within 8 Hours after Symptom Onset in Ischemic Stroke. New England Journal of Medicine 372, 2296–2306, (2015). [PubMed: 25882510]
8. Campbell BCV et al. Endovascular Therapy for Ischemic Stroke with Perfusion-Imaging Selection. New England Journal of Medicine Epub, (2015).
9. Powers WJ et al. 2015 AHA/ASA Focused Update of the 2013 Guidelines for the Early Management of Patients With Acute Ischemic Stroke Regarding Endovascular Treatment: A Guideline for Healthcare Professionals From the American Heart Association/American Stroke Association. Stroke; a journal of cerebral circulation, (2015).

10. Sakuma T, Leong-Poi H, Fisher NG, Goodman NC & Kaul S Further insights into the no-reflow phenomenon after primary angioplasty in acute myocardial infarction: the role of microthromboemboli. J Am Soc Echocardiogr 16, 15–21, (2003). [PubMed: 12514630]
11. Bekkers SC, Yazdani SK, Virmani R & Waltenberger J Microvascular obstruction: underlying pathophysiology and clinical diagnosis. J Am Coll Cardiol 55, 1649–1660, (2010). [PubMed: 20394867]
12. Broderick JP et al. Endovascular Therapy after Intravenous t-PA versus t-PA Alone for Stroke. New England Journal of Medicine 368, 893–903, (2013). [PubMed: 23390923]
13. Jayaraman MV, Grossberg JA, Meisel KM, Shaikhouni A & Silver B The clinical and radiographic importance of distinguishing partial from near-complete reperfusion following intra-arterial stroke therapy. AJNR. American journal of neuroradiology 34, 135–139, (2013). [PubMed: 22837313]
14. Alexandrov AV et al. Ultrasound-enhanced systemic thrombolysis for acute ischemic stroke. N Engl J Med 351, 2170–2178, (2004). [PubMed: 15548777]
15. Alexandrov AV et al. A pilot randomized clinical safety study of sonothrombolysis augmentation with ultrasound-activated perflutren-lipid microspheres for acute ischemic stroke. Stroke; a journal of cerebral circulation 39, 1464–1469, (2008).
16. Dinia MR, Ribo M, Santamarina E, Maisterra O, Delgado-Mederos R, & Alvarez-Sabin J, M. J, Molina C,. Timing of microbubble-enhanced sonothrombolysis strongly predicts intracranial haemorrhage in acute ischaemic stroke. European Stroke Conference, (2008).
17. Molina CA et al. Microbubble administration accelerates clot lysis during continuous 2-MHz ultrasound monitoring in stroke patients treated with intravenous tissue plasminogen activator. Stroke; a journal of cerebral circulation 37, 425–429, (2006).
18. Molina CA et al. Transcranial ultrasound in clinical sonothrombolysis (TUCSON) trial. Annals of neurology 66, 28–38, (2009). [PubMed: 19670432]
19. Wu J Theoretical study on shear stress generated by microstreaming surrounding contrast agents attached to living cells. Ultrasound Med Biol 28, 125–129, (2002). [PubMed: 11879959]
20. Marmottant P & Hilgenfeldt S Controlled vesicle deformation and lysis by single oscillating bubbles. Nature 423, 153–156, (2003). [PubMed: 12736680]
21. Marmottant P, Versluis M, de Jong N, Hilgenfeldt S & Lohse D High-speed imaging of an ultrasound-driven bubble in contact with a wall: “Narcissus” effect and resolved acoustic streaming. Exp Fluids 41, 147–153, (2006).
22. Longuet-Higgins MS Viscous streaming from an oscillating spherical bubble. Proceedings of the Royal Society of London A: Mathematical, Physical and Engineering Sciences 454, 725–742, (1998).
23. Yueh-Hsun C, Po-Wen C & Pai-Chi L Combining radiation force with cavitation for enhanced sonothrombolysis. Ultrasonics, Ferroelectrics and Frequency Control, IEEE Transactions on 60, (2013).
24. Dayton P, Allen J & Ferrara K The magnitude of radiation force on ultrasound contrast agents. Journal of the Acoustical Society of America 112, 2183–2192, (2002). [PubMed: 12430830]
25. Shortencarier MJ et al. A method for radiation-force localized drug delivery using gas-filled lipospheres. IEEE Trans Ultrason Ferroelectr Freq Control 51, 822–831, (2004). [PubMed: 15301001]
26. Brujan E-A & Matsumoto Y Collapse of micrometer-sized cavitation bubbles near a rigid boundary. Microfluidics and Nanofluidics 13, 957–966, (2012).
27. Brujan EA, Ikeda T & Matsumoto Y Jet formation and shock wave emission during collapse of ultrasound-induced cavitation bubbles and their role in the therapeutic applications of high-intensity focused ultrasound. Phys Med Biol 50, 4797–4809, (2005). [PubMed: 16204873]
28. Chen JL, Dhanaliwala AH, Dixon AJ, Klibanov AL & Hossack JA Synthesis and Characterization of Transiently Stable Albumin-Coated Microbubbles via a Flow-Focusing Microfluidic Device. Ultrasound in Medicine and Biology 40, 400–409, (2014). [PubMed: 24342914]
29. Dixon AJ, Dhanaliwala AH, Chen JL & Hossack JA Enhanced intracellular delivery of a model drug using microbubbles produced by a microfluidic device. Ultrasound in medicine & biology 39, 1267–1276, (2013). [PubMed: 23643062]

30. Dixon AJ, Rickel JMR, Shin BD, Klibanov AL & Hossack JA In Vitro Sonothrombolysis Enhancement by Transiently Stable Microbubbles Produced by a Flow-Focusing Microfluidic Device. Ann Biomed Eng 46, 222–232, (2018). [PubMed: 29192346]
31. Li L & Zuo Z Isoflurane preconditioning improves short-term and long-term neurological outcome after focal brain ischemia in adult rats. Neuroscience 164, 497–506, (2009). [PubMed: 19679170]
32. Wu JH & Diamond SL Tissue plasminogen activator (tPA) inhibits plasmin degradation of fibrin. A mechanism that slows tPA-mediated fibrinolysis but does not require alpha 2-antiplasmin or leakage of intrinsic plasminogen. J Clin Invest 95, 2483–2490, (1995). [PubMed: 7769094]
33. Marler J Tissue Plasminogen Activator for Acute Ischemic Stroke. New England Journal of Medicine 333, 1581–1588, (1995). [PubMed: 7477192]
34. Daffertshofer M et al. Efficacy of sonothrombolysis in a rat model of embolic ischemic stroke. Neuroscience Letters 361, 115–119, (2004). [PubMed: 15135907]
35. Dhanaliwala AH et al. In vivo imaging of microfluidic-produced microbubbles. Biomed Microdevices 17, 23, (2015). [PubMed: 25663444]
36. Fan Z, Liu H, Mayer M & Deng CX Spatiotemporally controlled single cell sonoporation. Proceedings of the National Academy of Sciences of the United States of America 109, 1–4, (2012).
37. Helfield B, Chen X, Watkins SC & Villanueva FS Biophysical insight into mechanisms of sonoporation. Proc Natl Acad Sci U S A, (2016).
38. van Wamel A et al. Vibrating microbubbles poking individual cells: drug transfer into cells via sonoporation. Journal of controlled release : official journal of the Controlled Release Society 112, 149–155, (2006). [PubMed: 16556469]
39. Choi JJ et al. Microbubble-size dependence of focused ultrasound-induced blood-brain barrier opening in mice in vivo. IEEE transactions on bio-medical engineering 57, 145–154, (2010). [PubMed: 19846365]
40. Borrelli MJ et al. Influences of microbubble diameter and ultrasonic parameters on in vitro sonothrombolysis efficacy. Journal of vascular and interventional radiology : JVIR 23, 1677–1684.e1671, (2012). [PubMed: 23106936]
41. Garstecki P et al. Formation of monodisperse bubbles in a microfluidic flow-focusing device. Applied Physics Letters 85, 2649–2651, (2004).
42. Hettiarachchi K, Talu E, Longo ML, Dayton PA & Lee AP On-chip generation of microbubbles as a practical technology for manufacturing contrast agents for ultrasonic imaging. Lab on a Chip 7, 463, (2007). [PubMed: 17389962]
43. Talu E et al. Maintaining monodispersity in a microbubble population formed by flow-focusing. Langmuir : the ACS journal of surfaces and colloids 24, 1745–1749, (2008). [PubMed: 18205422]
44. Kim J et al. Intravascular forward-looking ultrasound transducers for microbubble-mediated sonothrombolysis. Sci Rep 7, 3454, (2017). [PubMed: 28615645]
45. Kilroy JP et al. Reducing Neointima Formation in a Swine Model with IVUS and Sirolimus Microbubbles. Annals of Biomedical Engineering In Press, (2015).
46. Rickel JMR, Dixon AJ, Klibanov AL & Hossack JA A flow focusing microfluidic device with an integrated Coulter particle counter for production, counting and size characterization of monodisperse microbubbles. Lab Chip 18, 2653–2664, (2018). [PubMed: 30070301]
47. Dixon AJ et al. Microbubble-mediated intravascular ultrasound imaging and drug delivery. IEEE Transactions on Ultrasonics, Ferroelectrics, and Frequency Control 62, 1674–1685, (2015).
48. Porter TR et al. The Thrombolytic Effect of Diagnostic Ultrasound-Induced Microbubble Cavitation in Acute Carotid Thromboembolism. Invest Radiol 52, 477–481, (2017). [PubMed: 28383307]
49. Mathias W Jr. et al. Diagnostic Ultrasound Impulses Improve Microvascular Flow in Patients With STEMI Receiving Intravenous Microbubbles. J Am Coll Cardiol 67, 2506–2515, (2016). [PubMed: 27230046]
50. Gao S et al. Improvements in cerebral blood flow and recanalization rates with transcranial diagnostic ultrasound and intravenous microbubbles after acute cerebral emboli. Invest Radiol 49, 593–600, (2014). [PubMed: 24691139]

51. Schleicher N et al. Sonothrombolysis with BR38 Microbubbles Improves Microvascular Patency in a Rat Model of Stroke. PLoS ONE 11, e0152898, (2016). [PubMed: 27077372]

52. Helps SC, Meyer-Witting M, Reilly PL & Gorman DF Increasing doses of intracarotid air and cerebral blood flow in rabbits. Stroke 21, 1340–1345, (1990). [PubMed: 2396272]

53. Postema M, Marmottant P, Lancee CT, Hilgenfeldt S & de Jong N Ultrasound-induced microbubble coalescence. Ultrasound Med Biol 30, 1337–1344, (2004). [PubMed: 15582233]

54. Schwamm LH et al. Temporal Trends in Patient Characteristics and Treatment With Intravenous Thrombolysis Among Acute Ischemic Stroke Patients at Get With the Guidelines-Stroke Hospitals. Circ Cardiovasc Qual Outcomes, (2013).

55. Crumrine RC et al. Intra-arterial administration of recombinant tissue-type plasminogen activator (rt-PA) causes more intracranial bleeding than does intravenous rt-PA in a transient rat middle cerebral artery occlusion model. Experimental & translational stroke medicine 3, 10, (2011). [PubMed: 21933438]

56. Dixon AJ & Hossack JA Method and apparatus for accelerated disintegration of blood clot. United States of America Patent US9895158 (2018).

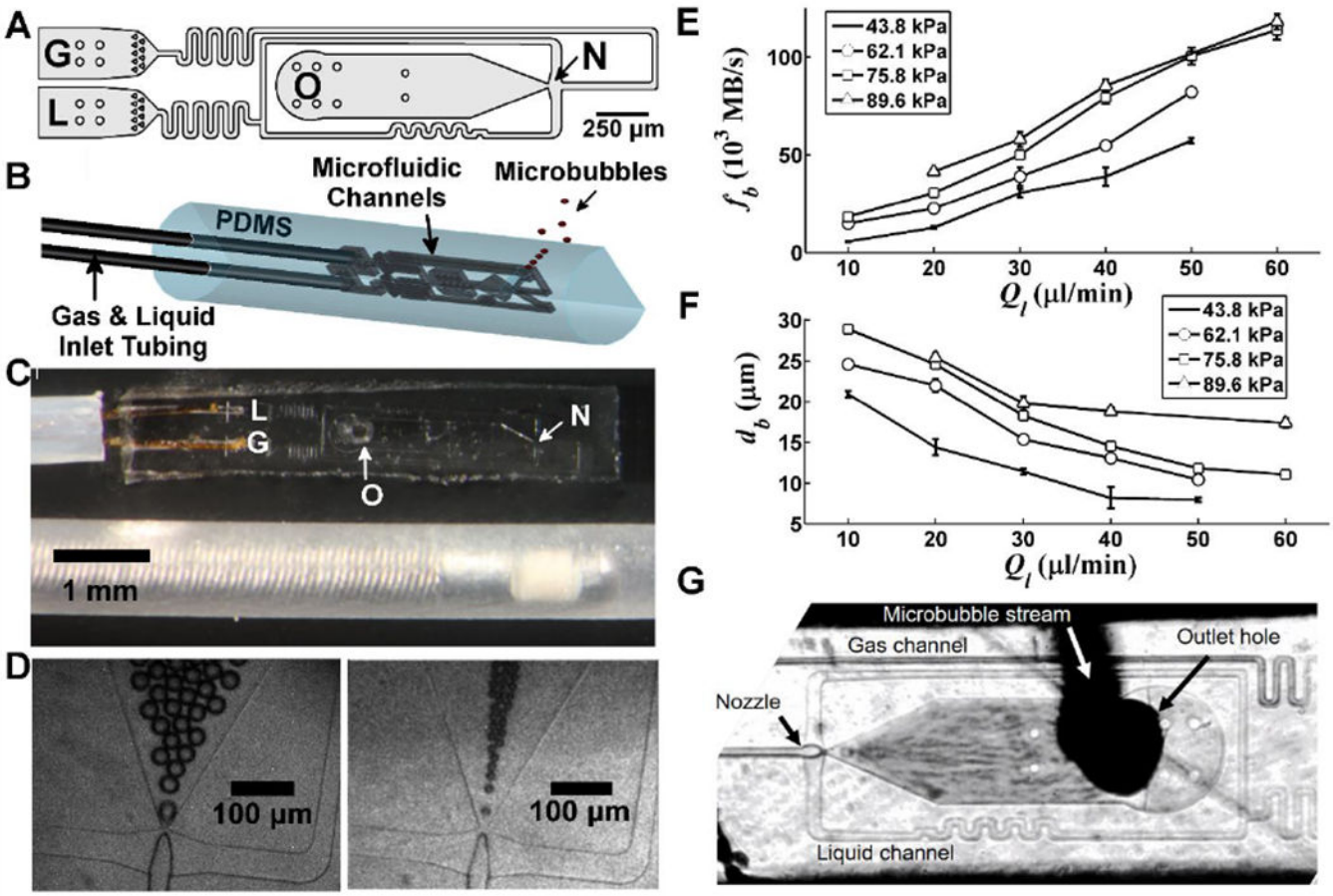

Figure 1: Catheter-based FFMD for microbubble production.

A) Schematic of photolithography mold. Abbreviations: G: gas inlet, L: liquid inlet, N: nozzle, O: outlet. The nozzle was approximately 8 µm wide, all channel widths were 25 µm wide, with the exception of the liquid channels that flare to 50 µm wide as they approach the nozzle. B) Three-dimensional model of PDMS-based catheter FFMD. C) Fabricated PDMS FFMD. Note the brown colored polyimide coated inlet tubing. Abbreviations same as in (A). D) High speed camera images of the FFMD producing microbubbles of 25 and 9 µm diameter. E) Production rate curves as a function of flow rate for varying gas pressures. F) Diameter curves as a function of flow rate for varying gas pressures. G) Camera image take at 60 FPS of the device in operation. Note the black stream of microbubbles exiting through the outlet hole.

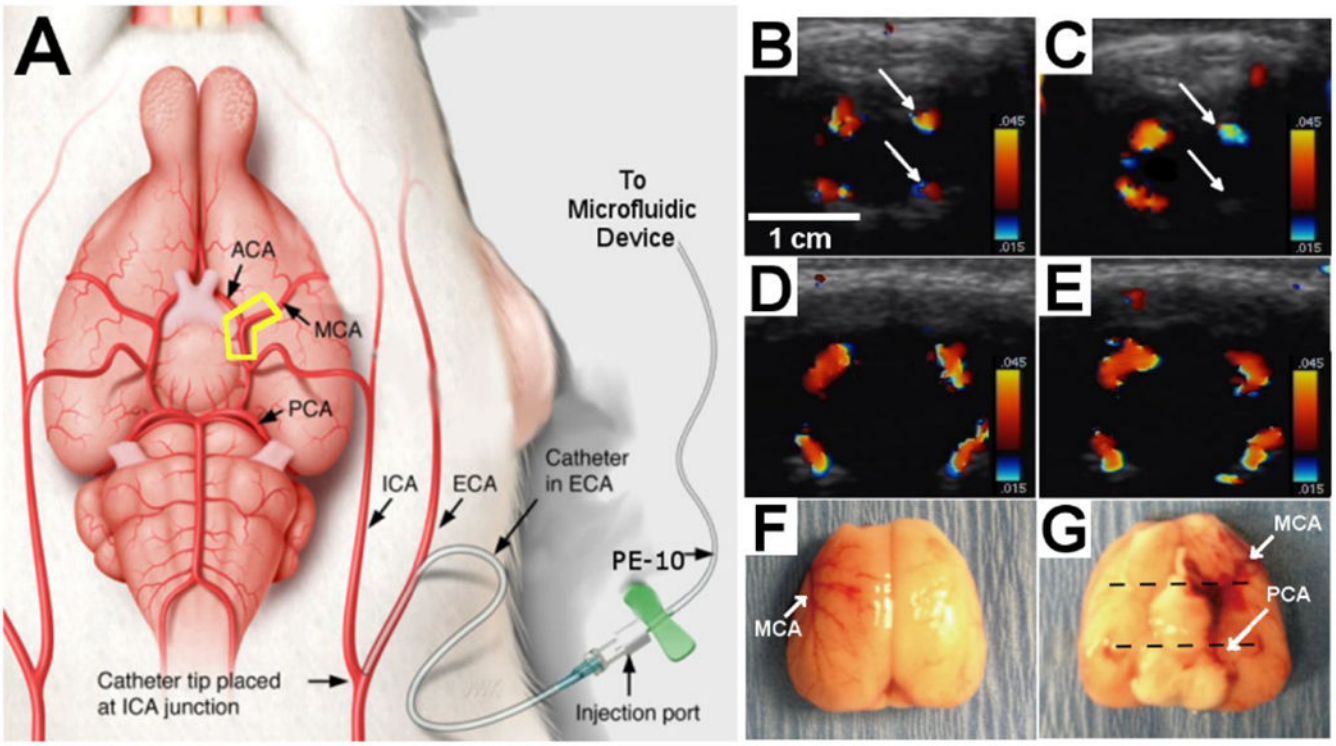

Figure 2: Rat ischemic stroke model.

A) Schematic of the catheterization surgery. The ECA was catheterized and a PE-10 tube was advanced to sit at the ICA junction. The PE-10 tube was used to administer the clot through the ICA, which lodged at the location outlined in yellow, at the junction of the Circle of Willis and the MCA. In the sonothrombolysis experiments, the microbubbles were administered through the same PE-10 tube. B-E). Doppler ultrasound images of the MCA (B,C) and PCA (D,E) before (left) and after (right) clot placement. Note the reduced flow measured in the MCA (C) but relatively unaffected flow in the PCA (E). F) Excised brain showing full occlusion of MCA and its distal vascular bed. G) Excised brain showing location of clot lodged at the junction of the Circle of Willis and the MCA. [Figure (A) adapted and modified from Crumrine RC *et al*[55] under the guidelines of the Creative Commons Public License (CCPL) 2.0 for Open Access Images.]

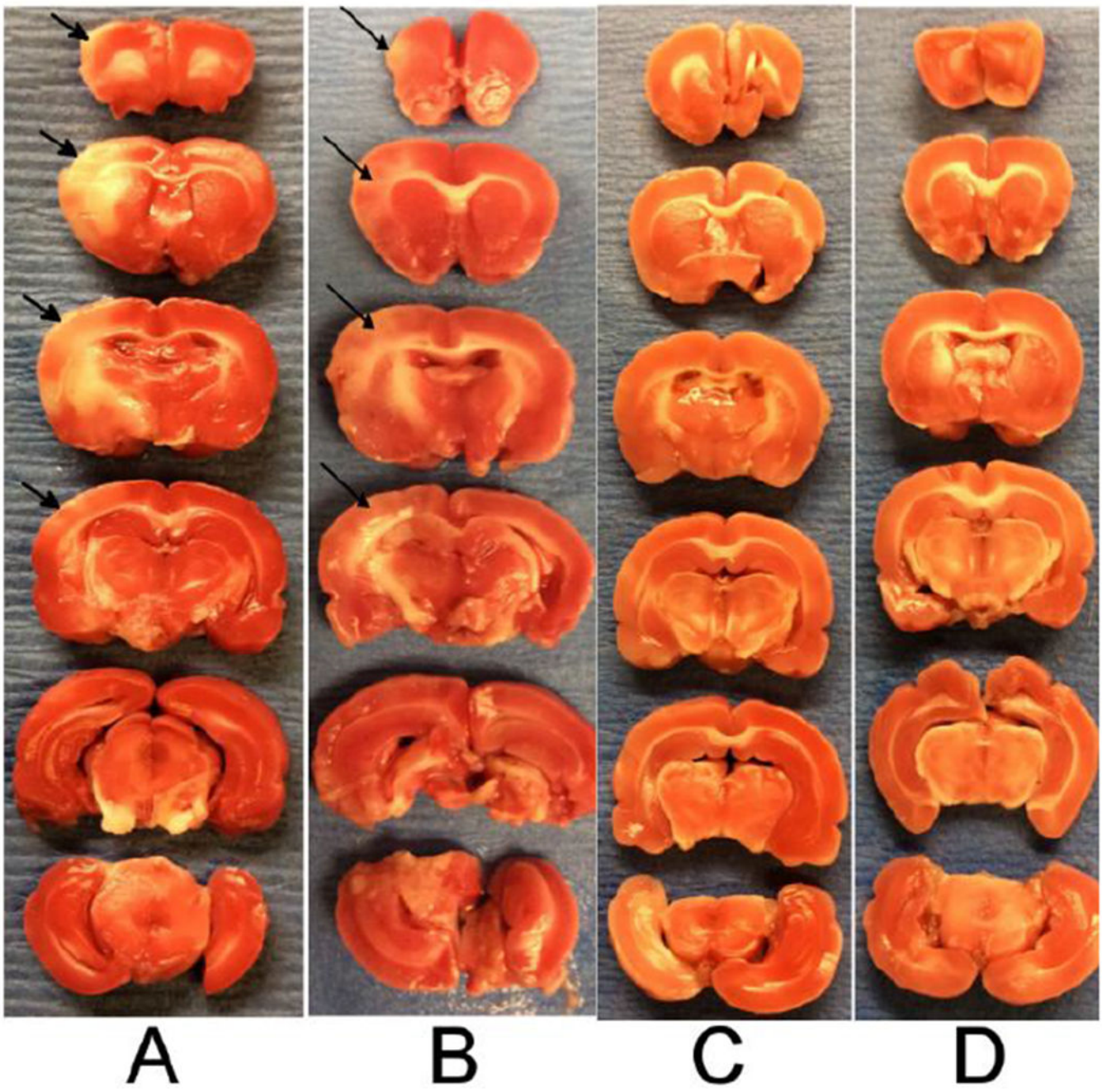

Figure 3: TTC staining of brains in safety study groups.

Infarct is identified by pale areas denoted by the black arrows. These TTC brain cross-sections are representative results of animals in the high-dose (A), medium-dose (B), low-dose (C), and control (D – no MBs) groups. Significant gas embolism resulted in group A, which led to lasting infarct and brain tissue loss.

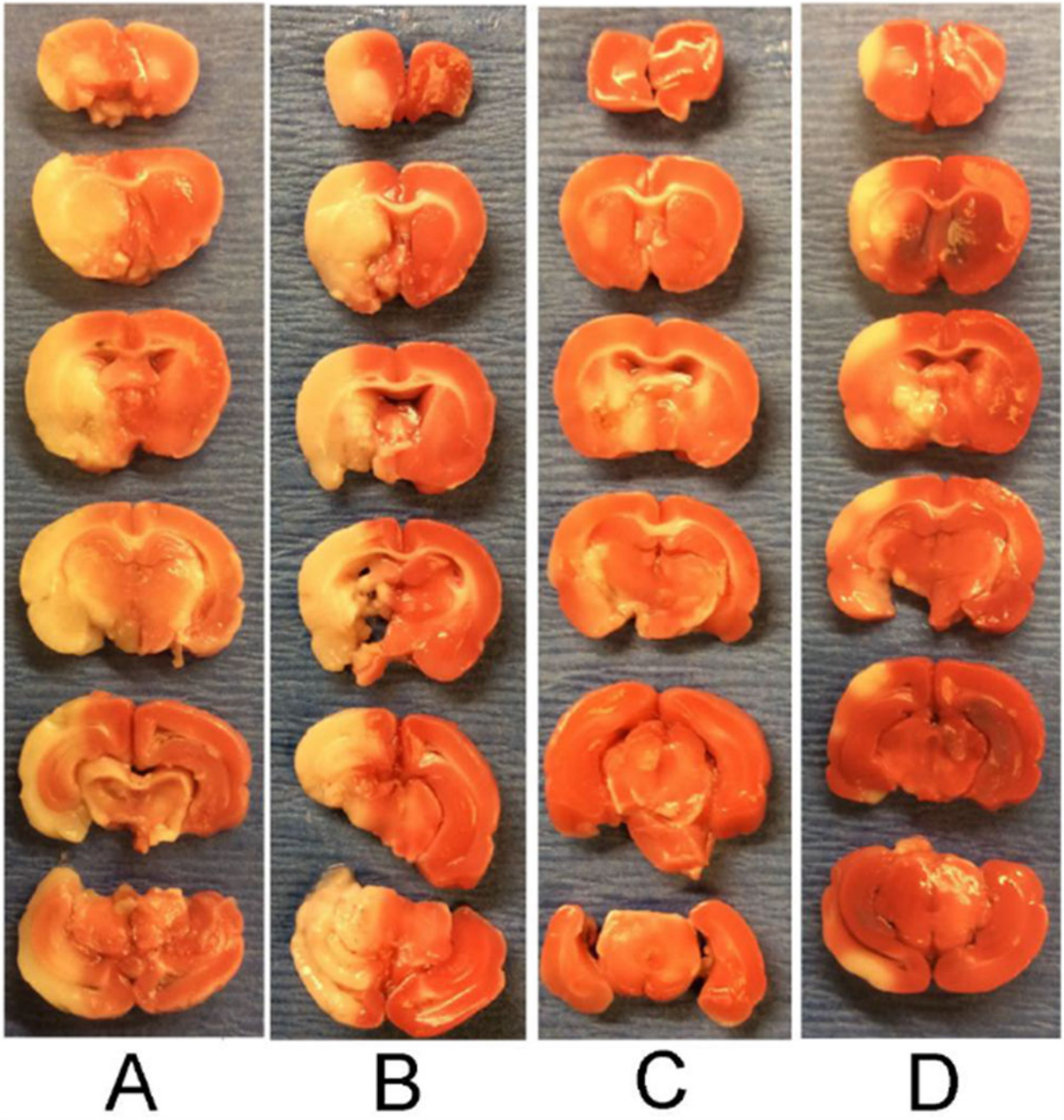

Figure 4: TTC staining of brains in sonothromboysis study groups.
Infarct is identified by pale colored areas. These TTC brain cross-sections are representative results of animals in the control group (A), low-dose rtPA group (B), high-dose rtPA group (C), and sonothrombolysis plus low-dose rtPA group (D). Note less infarction between group B and D despite receiving the same dose of intravenous rtPA.

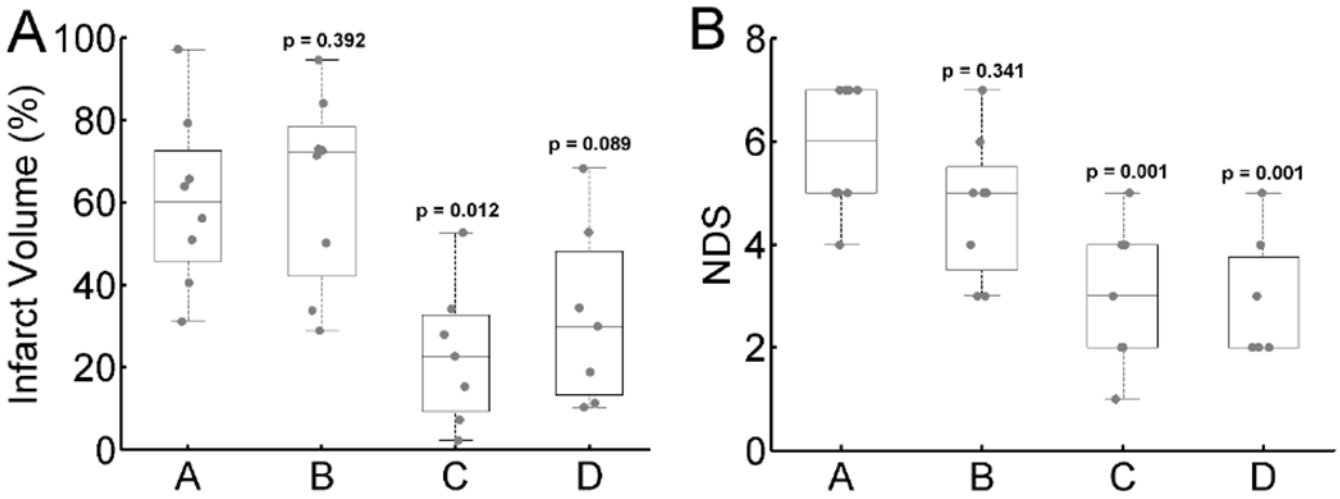

Figure 5: Boxplots of outcomes of the sonothrombolysis study.

A) Infarct volume across study groups and B) neurological deficit scores across study groups. *p*-values denote the comparison between the control group (Group A) and each of the other groups. Additional, *p* values for other comparisons are listed in the results section.

Table 1:

Summary of experimental groups in sonothrombolysis experiment

Group	N	rtPA (mg/kg)	Ultrasound	Microbubbles	Production Rate (MB/s)	Diameter (μm)
A	8	0	No	No	N/A	N/A
B	8	0.09	No	No	N/A	N/A
C	8	0.9	No	No	N/A	N/A
D	8	0.09	Yes	Yes	250×10^3	10 – 20